



## Article

# Monitoring of Khorasan (*Triticum turgidum* ssp. *Turanicum*) and Modern Kabot Spring Wheat (*Triticum aestivum*) Varieties by UAV and Sensor Technologies under Different Soil Tillage

Kristýna Balážová <sup>1,\*</sup>, Jan Chyba <sup>1,\*</sup>, Jitka Kumhálová <sup>2</sup>, Jiří Mašek <sup>1</sup> and Stanislav Petrásek <sup>1</sup>

<sup>1</sup> Department of Agricultural Machines, Faculty of Engineering, Czech University of Life Sciences, Kamýcká 129, 165 21 Suchdol, Czech Republic; masekj@tf.czu.cz (J.M.); petrasek@tf.czu.cz (S.P.)

<sup>2</sup> Department of Machinery Utilization, Faculty of Engineering, Czech University of Life Sciences, Kamýcká 129, 165 21 Suchdol, Czech Republic; kumhalova@tf.czu.cz

\* Correspondence: balazovak@tf.czu.cz (K.B.); chyba@tf.czu.cz (J.C.); Tel.: +420-224-383-137 (K.B. & J.C.)

**Abstract:** Khorasan wheat (*Triticum turgidum* ssp. *turanicum* (Jakubz.)) is an ancient tetraploid spring wheat variety originating from northeast parts of Central Asia. This variety can serve as a full-fledged alternative to modern wheat but has a lower yield than modern varieties. It is commonly known that wheat growth is influenced by soil tillage technology (among other things). However, it is not known how soil tillage technology affects ancient varieties. Therefore, the main objective of this study was to evaluate the influence of different soil tillage technologies on the growth of the ancient Khorasan wheat variety in comparison to the modern Kabot spring wheat (*Triticum aestivum*) variety. The trial was arranged in six small plots, one half of which was sown by the Khorasan wheat variety and the other half of which was sown by the Kabot wheat variety. Three soil tillage methods were used for each cultivar: conventional tillage (CT) (20–25 cm), minimum tillage (MTC) with a coulter cultivator (15 cm), and minimization tillage (MTD) with a disc cultivator (12 cm). The soil surface of all of the variants were leveled after tillage (harrows & levelling bars). An unmanned aerial vehicle with multispectral and thermal cameras was used to monitor growth during the vegetation season. The flight missions were supplemented by measurements using the GreenSeeker hand-held sensor and plant and soil analysis. The results showed that the Khorasan ancient wheat was better suited the conditions of conventional tillage, with low values of bulk density and high values of total soil porosity, which generally increased the nutritional value of the yield in this experimental plot. At the same time, it was found that this ancient wheat does not deplete the soil. The results also showed that the trend of developmental growing curves derived from different sensors was very similar regardless of measurement method. The sensors used in this study can be good indicators of micronutrient content in the plant as well as in the grains. A low-cost RGB camera can provide relevant results, especially in cases where equipment that is more accurate is not available.



**Citation:** Balážová, K.; Chyba, J.; Kumhálová, J.; Mašek, J.; Petrásek, S. Monitoring of Khorasan (*Triticum turgidum* ssp. *Turanicum*) and Modern Kabot Spring Wheat (*Triticum aestivum*) Varieties by UAV and Sensor Technologies under Different Soil Tillage. *Agronomy* **2021**, *11*, 1348. <https://doi.org/10.3390/agronomy11071348>

Academic Editor: Giovanni Caruso

Received: 27 May 2021

Accepted: 28 June 2021

Published: 30 June 2021

**Publisher's Note:** MDPI stays neutral with regard to jurisdictional claims in published maps and institutional affiliations.

**Keywords:** Khorasan wheat; unmanned aerial vehicle; soil tillage; spectral indices; GreenSeeker handheld crop sensor



**Copyright:** © 2021 by the authors. Licensee MDPI, Basel, Switzerland. This article is an open access article distributed under the terms and conditions of the Creative Commons Attribution (CC BY) license (<https://creativecommons.org/licenses/by/4.0/>).

## 1. Introduction

Tillage is an important process that affects soil properties such as the temperature, moisture content, bulk density, or stability of soil aggregates [1]. The method of processing and habitat conditions give soil a specific value that determines the growth, development, and yield of crops [2]. Conventional soil tillage, which is still the most commonly used method, is one of the most demanding tilling operations, as its depth is most often between 20 and 25 cm [3]. The disadvantage of this tillage method is that it can adversely affect the structure of the soil due to the increased disturbance of soil aggregates [4]. Conventional tillage with moldboard ploughing (25–28 cm depth) followed by spring tine harrowing compared to reduced tillage (two harrowings with spring tine harrows up to 4–6 cm depth

and sowing) has a worsening effect on the soil. This means reduced organic matter, poorer soil structure, reduced aggregate content, and increased bulk density [5]. Bilalis et al. [6] evaluated a field experiment comparing the influence of three different tillage methods (conventional, minimization, and no-till) on the quality, yield, and growth of four varieties of wheat ('Siette', 'Panifor', 'Myrto', and 'Estero'). The minimum tillage and no-till methods had the best effects on the soil (porosity and total nitrogen) while the highest grain yield was shown through the use of conventional tillage (CT) with the 'Siette', 'Myrto', and 'Estero' varieties, while the 'Panifor' variety had the highest yield after the use of minimization tillage. Grandy et al. [7] compared ploughing tillage to a depth of 30 cm with a no-till system. If the strategies and conditions for the habitat are chosen correctly, no-till can achieve the same results or even better results than conventional tillage. In the EU, ecological systems are becoming increasingly popular than conventional ones, with the share of ecologically managed land amounting to around 4% [8]. In the Czech Republic, conventional tillage predominates, mostly in areas rich in precipitation. In 2016, 66.5% of arable land was cultivated with conventional technology, 32.1% with conservation technology, and 1.4% with zero tillage [9]. The influence of different tillage on winter wheat yield at three locations in the Czech Republic during 6 seasons showed that the reduced tillage system combined with a high input level achieved higher yields for all wheat varieties than conventional tillage [10].

Wheat is among one of the biggest strategic agriculture crops around the world. Wheat has been the staple food of the population for more than 8000 years [11]. With a growing population, the demand for wheat will increase by up to 70% by 2050. This will mainly be due to a change in the eating habits of a growing population and climate change [12]. The original civilizations in Europe, West Asia, and Africa grew ancient wheat, which is now terminologically called einkorn, emmer, khorasan, and spelt. These are varieties bred from either wild or ancient wheat. Recently, the popularity of these natural varieties has been growing, mainly due to the allegedly better tolerance of people who are allergic to modern wheat [13,14] and protection against the development of type-2 diabetes [15]. Khorasan wheat (*Triticum turgidum* ssp. *turanicum*) has a registered trademark KAMUT®. The KAMUT® trademark must meet given specifications, especially regarding the nutritional properties of the grain and its growing conditions, which are focused on organic cultivation [16].

Differences in plant growth, which are also sometimes due to the response to the tillage technology used, can be assessed by modern monitoring systems. Platforms for crop monitoring provide either remote or proximal sensing. Remote sensing platforms can be distinguished according to the operative height from which the crop canopy is scanned. Optical remote sensing includes traditional satellite systems for monitoring natural resources such as Landsat or Sentinel 2. Using satellite images, it is only possible to yield predictions on larger plots [17–19]. However, these satellite images are still insufficient for objectives such as breeding experiments or plant health monitoring, where there is a very high demand for spatial accuracy.

With the technical progress of the past two decades, it has become possible to obtain images from unmanned aerial vehicles, which have a very high spatial resolution and can thus monitor the crop canopy with very high accuracy [20]. Another advantage in comparison to satellite images is the flexibility of the acquisition time and the ability to focus on selected phenological phases of the monitored stands. Another advantage of modern unmanned aerial vehicles (UAVs) is the ability to acquire images with several sensors simultaneously, for example, thermal images are supplemented by multispectral images [21].

Proximal sensors such as the GreenSeeker handheld crop sensor can be used for nitrogen uptake monitoring, yield prediction, and thus for determining site-specific nitrogen management strategies in wheat [22]. The GreenSeeker handheld crop sensor is not suitable for measuring the normalized difference vegetation index (NDVI) status of medium and large agricultural fields due to the demands of data collection and processing to obtain the

resulting map [23]. On the other hand, Ali et al. [22] found that GreenSeeker can give better information regarding crop canopy than contact sensors, which measure greenness on one spot on a leaf. Proximal sensors can find a better application in the regular monitoring of smaller agricultural plots, as in the case of the Naser et al. [24] study.

Sensors mounted on the platforms described above can provide an image in a minimum of one spectral band up to several spectral bands in various wavelength ranges. A multispectral camera is usually used for crop status monitoring and can be used to determine aspects such as structure, vigor, variability, or the chlorophyll content in leaves [25–29]. Thermal images can provide information on the condition of crops damaged by drought [30]. The spectral resolution of a thermal camera normally ranges from 7 to 14  $\mu\text{m}$  in one spectral band [31].

Crop canopy status is usually expressed by vegetation indices as the ratio of difference in the sums of the sensor measurements, usually in two or more bands based on the strong reflectance in the near infrared part and strong absorption in red part of the electromagnetic spectrum [32]. The NDVI is one of the longest used vegetation indices, with its origins dating back to 1974 [33]. This index is used as a reliable tool to determine and evaluate the structure, vitality, health, and other biophysical parameters of agricultural crops [34–36]. The main advantage of this index is its easy readability and orientation in the determined values. In general, values lower than 0.25 signal bare soil. Higher values indicate varying degrees of vitality and crop canopy coverage, which is important, for example, in the tillering growth stage [37]. The NDVI alternative for the estimation of chlorophyll in leaves is the green normalized vegetation index (GNDVI) developed by Gitelson et al. [38], which uses the near-infrared and green electromagnetic parts of the spectrum in various ratios for chlorophyll content estimation. The usability of the GNDVI index was proven using corn, garlic, oats, onions, potatoes, sunflowers, alfalfa, and grapevines [39]. The triangular greenness index (TGI) spectral index [40] can fully serve the same purposes as NDVI or GNDVI if only images in the visible part of the spectrum are available [41]. Some authors, Gitelson & Merzlyak [42] or Xie et al. [43], for example, found through their research that vegetation indices with the red-edge part of the electromagnetic spectrum can be sensitive to leaf chlorophyll, as can the traditional VIs. The advantage of the red edge bands is using the relatively narrow part of the electromagnetic spectrum that relates to a position between the red absorption maximum and near infra-red high reflectance. Xie et al. [43] mentioned that the chlorophyll index green (CIG; [44]) has a close relationship to both chlorophyll content and leaf area index (LAI; [45]), but the chlorophyll index red edge (CIR; [46]) is more sensitive to small changes in the canopy, gap fraction, and senescence [47]. Using red-edge bands, it is possible to capture its shift to longer wavelengths, which is usually caused by increasing chlorophyll content [48]. The CIG and CIR were used by the authors of Xie et al. [43] with the aim of analyzing how changes in chlorophyll content and LAI contribute to reflectance variability in the RED, NIR, and red-edge bands. They monitored the spectral properties of winter wheat, barley, alfalfa, and maize.

It is clear from the literature review that the influence of soil tillage technology to wheat growth was studied in the past. Nevertheless, there is no information from literature regarding this influence on the ancient Khorasan variety. Therefore, the main objectives of this study were to evaluate how different types of soil tillage technology can affect the growth and conditions of old Khorasan wheat compared to modern Kabot spring wheat and to assess the suitability of the methods used to measure the condition of the stand during the vegetation season.

## 2. Materials and Methods

### 2.1. Experimental Area and Soil Tillage

The study was conducted in the 2020 vegetation season and was located in six regular plots in the size of  $4 \times 50$  m near Čenovice ( $49^{\circ}47'42.78''$  N,  $15^{\circ}6'35.94''$  E), a central Bohemian region in the Czech Republic. The experimental area has a south-eastern aspect with a  $2.63^{\circ}$  slope and is 481 m a.s.l. on average. The soil is Haplic Luvisol. The soil classification (sampled from a depth of 5–10 cm) according to WRB (The World Reference Base) in percentages was clay 15.1%; silt 30.9%; very fine sand 9.2%; fine sand 14.3%; medium sand 12.1%; coarse sand 9.4%; very coarse sand 9%. Soil classification was performed on a Horiba LA-960 device (dry dispersion). Temperature and precipitation were measured by an agrometeorological station located next to the experiment. Table 1 lists the precipitation rates and temperatures for the observed 2020 cropping season for wheat varieties. Meteorological data are divided according to the main phenological stages on the BBCH scale [49]. Temperature values for the dates of UAV scanning are also given there.

**Table 1.** Precipitations and temperatures at different growth stages according to the BBCH scale recorded in the experimental field. Temperatures for dates of UAV scanning.

Growth Stages	Temperature (°C)	Precipitation (mm)
BBCH 0–19 (12 April (sowing)–9 May)	10.30	53.58
BBCH 20–29 (10 May–23 May)	10.94 (18.2 for 18 May)	42.93
BBCH 30–59 (24 May–30 June)	15.97 (18.4 for 11 June)	225.87
after 60 BBCH (after 1 July)	19.03 (20.9 for 2 July; 24.5 for 14 July)	75.09
Sum	-	397.47
Mean	14.06	99.37

The experimental area was divided into six plots. The size of one plot was  $4 \times 50$  m ( $200 \text{ m}^2$ ) with a 4 m wide handling gap between the parcels. Khorasan was sown in one-half of the trial area (plots 1–2–3) and the Kabot variety was sown in the other half (plots 4–5–6) of the experimental field. Three different soil tillage technologies were used for each section of the cultivar (Figure 1). Plots 1 and 4 were cultivated using conventional tillage (CT) with moldboard plowing at a depth of 20–25 cm. Plots 2 and 5 were cultivated by means of minimum tillage (MTC) using a coulter cultivator twice (at a depth of 15 cm). Plots 3 and 6 were cultivated using minimization tillage (MTD) with the use of a disc cultivator twice (at a depth of 12 cm). The soil surface for all variants was leveled with a harrows (4 cm) and leveling bars.

Sowing took place on 12.4.2020. After the levelling the soil surface using harrows, the NPK fertilizer was manually scattered on the individual plots at a rate of  $200 \text{ kg} \cdot \text{ha}^{-1}$  (4 kg per parcel). Further fertilization using NPK took place after the first measurement on 18.5 on 7.5. Mustang was applied against the developed dicotyledonous weeds. LAV fertilizer at a dose of  $200 \text{ kg} \cdot \text{ha}^{-1}$  was applied manually on 2.6. The harvest took place on 21 August 2020 and was completed using the FORTSCHRITT E516B combine harvester. The harvest took place on the individual plots. The combine harvester hopper was emptied onto an unfolded tarpaulin, and the contents of each plot were separated and weighed separately.

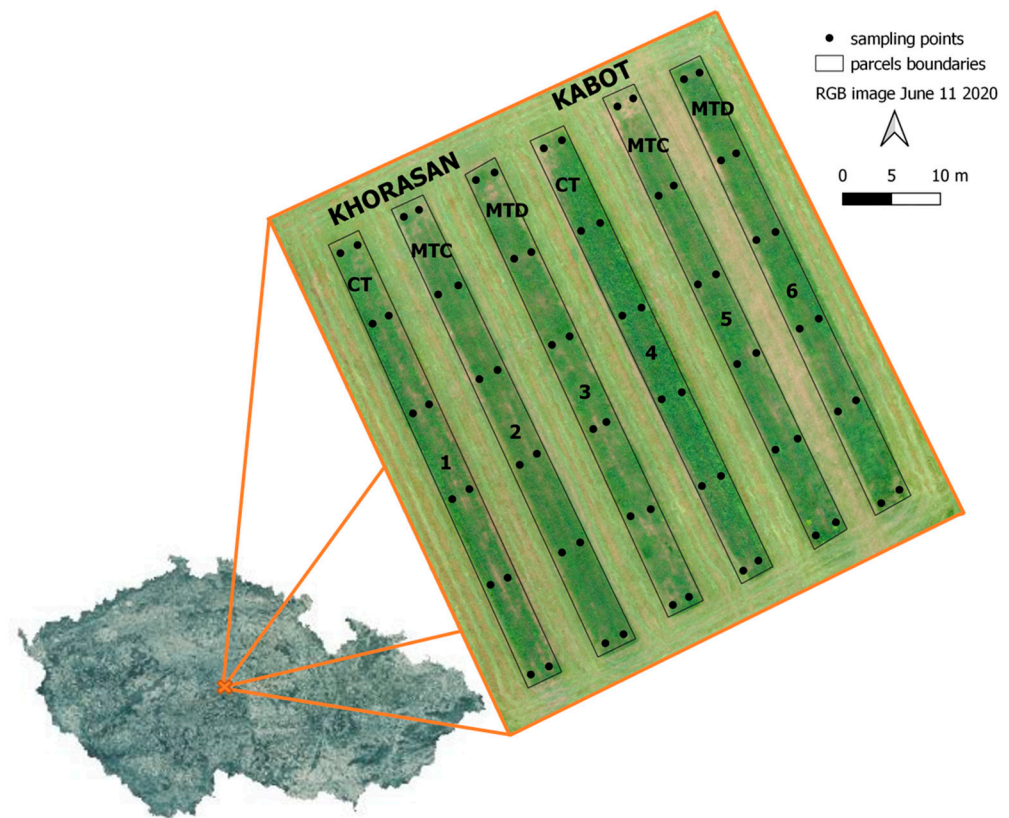


**Figure 1.** The experimental area divided according to variety and soil tillage technologies: conventional tillage (CT), minimum tillage (MTC), and minimization tillage (MTD).

## 2.2. UAV Canopy Sensing and Data Processing

Four flights were performed during the cropping season (see Table 1) using a fixed-wing eBeeX drone with a MicaSense RedEdge MX camera (AgEagle Aerial Systems Inc., Wichita, KN, USA) and a DuetT dual camera (senseFly SA, Route de Genève 38, Cheseaux-sur-Lausanne, Switzerland) comprising of a 20 Mpx RGB sensor with a 28 mm focal lens–S.O.D.A. camera and an infrared camera developed by FLIR technology for thermal mapping (details in Table 2).

**Table 2.** Center wavelengths for individual spectral bands and bandwidth of sensors used in this study.

Sensor/Camera	Blue (nm)	Green (nm)	Red (nm)	Red Edge (nm)	NIR (nm)	Thermal ( $\mu\text{m}$ )
MicaSense RedEdge MX	475 (20)	560 (20)	668 (10)	717 (10)	840 (40)	-
S.O.D.A./DuetT	450 (100)	520 (100)	660 (130)	-	-	-
IR sensor/DuetT	-	-	-	-	-	7.5–13.5
GreenSeeker	-	-	660 (25)	-	780 (25)	-

Each of the UAV missions were performed at the same hour, at about 1:00 p.m. (CET), with the aim to maintain consistent flight conditions. The average speed of the fixed wing was about  $11 \text{ m}\cdot\text{s}^{-1}$ . SW eMotion was used for flight planning and UAV control. The flight parameters and postflight processing differed based on the camera used. The flights using the Micasense RedEdge MX camera were arranged for 75% longitudinal and 75% lateral overlap (according to the producer guide and recommendations: <https://support.micasense.com/hc/en-us/articles/115000831714-How-to-Process-MicaSense-Sensor-Data-in-Pix4D>, accessed on 15 May 2021), and an 88 m flight height

(above elevation data) with a spatial resolution of  $6.0 \text{ cm} \cdot \text{px}^{-1}$  for the resulting images. The MicaSense Red Edge MX camera required radiometric calibration before and after each flight using a calibrated reflectance panel (CRP). The CRP made it possible to convert the raw pixel values from the RedEdge images to absolute reflectance. The information regarding the calibration was stored in the EXIF metadata and was available for further image processing. Flights with the DuetT camera were performed with 80% longitudinal and 75% lateral overlap and at 91.8 m above the elevation data flight altitude, with a  $12.0 \text{ cm} \cdot \text{px}^{-1}$  resulting spatial resolution for the thermal images. The S.O.D.A. camera had the following settings: 84% longitudinal and 83% lateral overlap and a resulting  $2.1 \text{ cm} \cdot \text{px}^{-1}$  spatial resolution for the RGB images. Accuracy was ensured by VRS.MAX-CZEPOS (master auxiliary stations, RTCM 3.1. correction format) provided by the CZEPOS service from the Czech Office for Surveying, Mapping and Cadastre of the Czech Republic. The resulting average accuracy of these missions was 4.8 cm horizontally and 5.2 cm vertically.

The images were pre-processed and refined in the postflight tool eMotion SW were uploaded into Pix4D SW (Pix4D S.A., Route de Renens 24, Prilly, Switzerland) and processed by a common procedure that consisted of several steps that ensured high accuracy of the resulting orthomosaic (details available at: <https://support.pix4d.com/hc/en-us/articles/202557759-Menu-Process-Processing-Options>, accessed on 15 May 2021). Images from Duet T thermal camera were processed using Duet T templates. The thermal maps were visualized in absolute temperature values. The resulting layers were in the GeoTIFF format georeferenced in the WGS84 UTM Zone 33N coordinate system.

The NDVI, GNDVI, CIR, and TGI (for images from S.O.D.A. and MicaSense camera) spectral indices and plant height, which derived from digital terrain model (DTM) and the digital surface model (DSM), were calculated for each of the data sets (details in Table 3). Plant height was computed from the RGB orthophoto as the difference between the DSM derived for each scanning term and the first scan date of the DTM, which was completed when the soil was best detectable.

**Table 3.** List of vegetation indices and parameters evaluated in this study.

Spectral Index	Algorithm	Developed by	References
Normalized Difference Vegetation Index (NDVI)	$(R_{\text{nir}} - R_{\text{red}})/(R_{\text{nir}} + R_{\text{red}})$	Biomass, structure, vigor	Rouse et al. (1974)
Green Normalized Difference Vegetation Index (GNDVI)	$(R_{\text{nir}} - R_{\text{green}})/(R_{\text{nir}} + R_{\text{green}})$	Chlorophyll	Gitelson et al. (1996)
Chlorophyll Index Red Edge (CIR)	$(R_{\text{nir}}/R_{\text{re}}) - 1$	Chlorophyll	Gitelson et al. (2005)
Triangular Greenness Index (TGI)	$R_{\text{green}} - 0.39 \times R_{\text{red}} - 0.61 \times R_{\text{blue}}$	Chlorophyll, nitrogen	Hunt et al. (2013)
Thermal IR index		Temperature ( $^{\circ}\text{C}$ )	
Height	DSM (t) – DTM	Computing plant height (m)	

$R_{\text{red}}$  = red reflectance;  $R_{\text{green}}$  = green reflectance;  $R_{\text{nir}}$  = near-infrared reflectance;  $R_{\text{re}}$  = red edge reflectance; DSM (t) = digital surface model derived from all dates of image acquisition; DTM = digital terrain model derived from the first scan date.

### 2.3. Proximal Canopy Sensing, Soil and Plant Sampling

The GreenSeeker (version 1.00, Rev B, 2012, Trimble Inc., Sunnyvale, CA, USA) was used to obtain the NDVI values directly above the selected areas of plant cover. The NDVI values were able to convert the information from the RED and NIR reflectance immediately into values of the NDVI spectral index [50]. Data were collected at 72 sampling points (see Figure 1) during the vegetation season for wheat varieties on 18 May, 11 June, 14 July, and 24 July.

Soil samples were put into physical cylinders in the form of undisturbed soil samples (Kopecky's cylinder) with a capacity of  $100 \text{ cm}^3$  from a depth of 5–10 cm. The evaluation was completed according to the Novak method [51]. The following characteristics were

evaluated from the samples: initial moisture content, bulk density, total porosity, capillary, and non-capillary porosity. Samples were taken three days after the wheat harvest.

Other soil samples were taken from a depth of 10–15 cm from each parcel after harvesting the grain on 21 August 2020. The samples were given to an external laboratory at the Crop Research Institute in Prague, where the necessary analyses were carried out. The samples identified the levels of accessible nutrients (P, K, Mg, Ca)—determined in the Mehlich III extractant, as well as the microelement content (B, Cu, Mn, Zn, Fe)—also specified in the Mehlich III extractant [52]. This method is the most widely used method to determine the content of nutrients or risk elements in the soil. Methodology: The soil sample (weigh 10 g) was shaken on a rotary shaker for 10 min into a sealable plastic container with a capacity (200–400) mL with the Mehlich III extractant (modification by Trávník et al. [53]). The Mehlich III extractant was composed of the following: 0.2 mol·L<sup>-1</sup> of concentrated acetic acid CH<sub>3</sub>COOH, 0.015 mol·L<sup>-1</sup> of ammonium fluoride solution NH<sub>4</sub>F, 0.013 mol·L<sup>-1</sup> HNO<sub>3</sub>, 0.25 mol·L<sup>-1</sup> of ammonium nitrate NH<sub>4</sub>NO<sub>3</sub>, and 0.001 mol·L<sup>-1</sup> of ethylenediaminetetraacetic acid EDTA in 1:10 ratio (*w:v*—10 g of soil and 100 ± 0.5 mL of extractant). After extraction, the suspension was immediately filtered through thick filter paper [54].

Whole plants were collected before the harvest date (21 August) from six selected locations of each parcel (more precisely, from sampling points where data was taken using the GreenSeeker) using electric scissors just above the ground. The area of each site was 0.25 m<sup>2</sup> (0.5 × 0.5 m). The locations were bound by a U-shaped rod. The number of spikes from the cut plants, the total weight of the spikes and the weight of a thousand seeds (WTS), and the content of macro and micronutrients in the grains were assessed. The plant samples were analyzed in an external laboratory at the Crop Research Institute in Prague.

#### 2.4. Statistical Analysis

The statistical analysis was processed in Statistica 13.5.0.17 software by TIBCO Software Inc., Tulsa, OK, USA. It was a mainly graphical processing of the resulting values as 2D graphs of averages and confidence intervals. There was also a statistical analysis, which specifically used the ANOVA tool and Tukey's HSD (honestly significant difference) test at the level of significance of 0.05. For basic data processing, MS Excel software was used. The zonal statistics tool in QGIS SW was used for image analysis.

### 3. Results and Discussion

#### 3.1. Evaluation of Soil Parameters under Different Tillage

Basic physical soil parameters (moisture content, bulk density, total porosity, capillary porosity, and non-capillary) are given in Table 4. The content of major macronutrients in the soil is reported in Table 5.

**Table 4.** Basic physical soil parameters (initial moisture content, bulk density, total porosity, capillary porosity, and non-cappillary porosity) for Khorasan and Kabot varieties and plots with different tillage methods (CT = conventional tillage; MTC = minimum tillage; MTD = minimization technique).

Variant	Varieties	Initial Moisture Content (Vol.%)	Bulk Density (g·cm <sup>-3</sup> )	Total Porosity (Vol.%)	Capillary Porosity (Vol.%)	Non-Capillary Porosity (Vol.%)
1 CT	Khorasan	20.21	1.35	48.97	26.12	9.58
2 MTC		24.69	1.42	46.29	26.89	8.76
3 MTD		18.09	1.37	48.35	27.31	10.66
4 CT	Kabot	20.67	1.36	48.68	27.34	8.15
5 MTC		26.27	1.45	45.30	27.91	9.10
6 MTD		21.82	1.38	48.10	28.55	10.59

**Table 5.** Content of macronutrients in soil (phosphorus, magnesium, potassium, and calcium) for Khorasan and Kabot varieties and plots with different tillage (CT = conventional tillage; MTC = minimum tillage; MTD = minimization technique).

Variant	Varieties	P (ppm)	Mg (ppm)	K (ppm)	Ca (ppm)
1 CT	Khorasan	62.8	159.3	72.9	1 803.9
2 MTC		67.3	106.3	65.4	1 531.9
3 MTD		59.2	105.5	89.6	1 342.3
4 CT	Kabot	52.9	88.7	50.6	1 503.7
5 MTC		47.8	102.7	57.0	1 427.1
6 MTD		42.7	123.5	62.2	1 471.7

The plots with the ancient Khorasan wheat variety contained a generally higher content of macronutrients in the soil (see Table 5). This fact is supported by various studies [41,44,55]. In general, this ancient wheat does not have demanding growing conditions, but at the same time, the grain is rich in nutrients compared to the modern Kabot variety. The results in Table 5 showed that the different tillage methods played a significant role in the ability of each individual variety to absorb nutrients and use them for growth. Khorasan wheat prospered better in conventionally tilled soil, where the bulk density of the soil was the smallest and the total porosity was the largest. From the point of view of the tillage variants, there are interesting results for the MTC variant, where the highest values of all the tillage variants were found for bulk density and initial moisture content (see Table 4).

### 3.2. Evaluation of Growth Parameters under Different Tillage

It can be seen in Table 6 that Khorasan wheat grains generally have higher values for both macro and micronutrients. Only the macronutrient potassium (K) shows no difference, and the values are variable. According to Wijngaard and Arendt [56], Khorasan wheat is classified as a healthy food due to its higher content of some nutrients, which agrees with this study. Likewise, Slavin et al. [57] point to a higher content of beneficial substances in the whole grains of Khorasan wheat. In addition, the interaction between all of the components, such as macro and micronutrients, omega 3-fatty acids, fiber, probiotic oligosaccharides, etc., gives these grains valuable nutritional value, which according to Maki and Phillips [58] can positively affect human health, as they can even reduce type 2 diabetes or the risk of obesity [13].

The development of the height of the wheat varieties and the yield parameters (number and total weight of spikes and weight of thousands of seeds) resulting from the different tillage methods are shown in Figure 2. The growth parameters of the selected wheat varieties cultivated under different tillage methods during the entire vegetation season were evaluated by spectral indices (Figure 3).

**Table 6.** Content of macronutrients (phosphorus (P), magnesium (Mg), potassium (K) and calcium (Ca)) and micronutrients (copper (Cu), zinc (Zn), iron (Fe), manganese (Mn) and boron (B)) in grains of the Khorasan and Kabot wheat varieties and plots with different soil tillage.

Variant	Varieties	%					ppm			
		P	Mg	K	Ca	Cu	Zn	Fe	Mn	B
1 CT	Khorasan	0.494	0.141	0.495	0.066	6.11	62.10	60.30	43.96	1.87
2 MTC		0.426	0.125	0.465	0.063	6.39	51.17	50.47	46.86	1.61
3 MTD		0.405	0.128	0.459	0.065	5.83	41.96	50.33	44.58	1.54
4 CT	Kabot	0.371	0.129	0.473	0.059	4.93	32.17	52.04	42.81	1.74
5 MTC		0.382	0.129	0.491	0.054	4.91	29.84	44.26	39.89	1.65
6 MTD		0.374	0.129	0.472	0.060	4.70	28.77	51.10	40.08	1.53

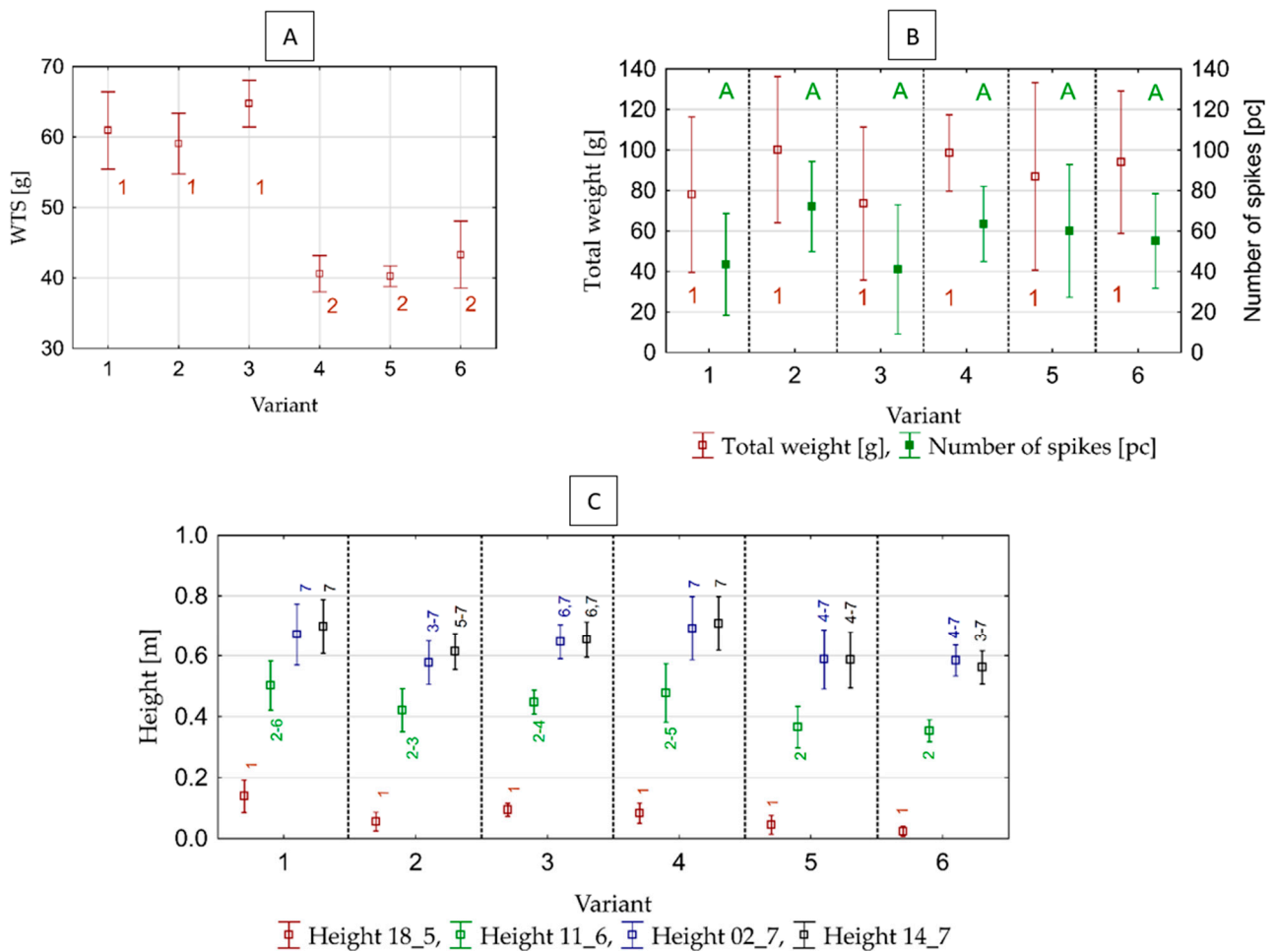


**Figure 2.** The development of the yield parameters: weight of thousands of seeds–WTS (A); number and total weight of spikes (B); and the height of wheat varieties (C) calculated as the difference between DSM (t) and DTM, where DSM (t) = digital surface model derived from all dates of image acquisition and DTM = digital terrain model derived from the first scan date from different soil tillage methods. Variants represent different types of tillage and varieties of wheat. Numbering 1,2,3 ... and letter A are homogenous groups according to Tukey’s HSD test,  $\alpha = 0.05$ .  $\square, \blacksquare$  Mean values for each parcel,  $I \pm 0.95$  conf. interval.

There are large differences in the weight of one thousand seeds (WTS) between the varieties. The Khorasan variety has a much higher average WTS than Kabot. Khorasan has large grains and a high WTS value (usually around 50 g). In the case of this study, WTS was 62 g on average, which is consistent with the study of Grausgruber et al. [59]. They stated that in some cases, the WTS could be higher than 60 g. Differences in WTS values were also evident in the tillage variants, especially for variants 3 and 6 (MTD), where there is an increase in average values. However, this is a statistically insignificant difference within the wheat varieties. Khorasan seemed to be much more sensitive to the soil conditions (compared to Table 4—soil parameters). On the other hand, the number of spikes and the total weight of the spikes have a diametrically different trend than WTS. With the increasing number of spikes on the plot, the WTS decreased, but the total weight of the spikes was higher because the spikes contained more seeds. Where there were fewer numbers of spikes, there were fewer number of shoots. The individual plants then had more space and more nutrients to help them grow and develop. Tari [60] found that wheat is sensitive to water access during the stem elongation and heading stages. A lack of water in these stages can lead to a decrease in yield. Our results indicate sufficient water during the stem elongation phase. However, soil tillage played a significant role in the availability of water and nutrients for the growth and the resulting yield in the case of both wheat

varieties. The number and weight of the spikes are in accordance with the trend in the soil capillary porosity.

Height was calculated from UAV images as DSM-DTM (see Table 3). During the tillering stage (18 May), the Khorasan variety crops were higher compared to the Kabot crops, indicating good germination and relatively good adaptation to the habitat conditions of this variety. Khorasan plants generally reach a higher height, most often around 127 cm [61]. The evaluation of the images also showed significant differences in plant height between the experimental parcels with different soil tillage. The tallest plants on all measurement dates for both varieties were the variant that was cultivated with conventional plowing technology (CT). These variants also had the highest total porosity and the lowest bulk density values (details in Table 4), which are the soil conditions most suitable for growth. Initial moisture content at the time of soil sampling was medium to low. On the contrary, the lowest Khorasan wheat height was found in the plot with minimum tillage; in the case of the Kabot wheat, the lowest height was found in the minimum and minimization tillage variants. Crop height for both varieties are in accordance with bulk density and has the of the opposite trend that can be seen in the total porosity values. The growth trends of varieties on plots with different tillage is steady. In the stages after BBCH 60 (2 and 14 July), the crops had already formed spikes, and the development of the grains in comparison with the WTS values is relatively well captured in Figure 2. Even though the WTS reached the highest value, the crop height in the last scanning (14 July) was lower than in the previous one (2 July). UAV height measurement is a relatively common and reliable method of capturing the vitality of the crop, along with derived spectral indices [62]. In the case of our measurements, we had a spatial resolution of about  $2 \text{ cm} \cdot \text{px}^{-1}$ , which is sufficient to derive a relatively accurate model.

The development of NDVI values calculated from the MicaSense camera related to individual plots and dates showed a very balanced trend, especially in the later crop scanning sessions (see details in Figure 3). During the first UAV scanning (18 May), the Kabot variety in a plot with conventional tillage was the most lively. The stand was the best involved here, it had the best tillering ability (higher capillary porosity and lower bulk density of soil). These results are in line with the number of spikes (see Figure 2). The Khorasan variety had relatively the same development on all three plots with different tillage. However, a plot with conventional tillage proved to be the most suitable for the Khorasan variety in terms of evaluation using the spectral indices. Conversely, Glamoclija et al. [63] stated that the Khorasan variety best benefits in worse soil conditions in mountainous areas. According to Rajčić [64], the quality and yield of grains are mainly affected by the climatic conditions of the habitat. Our findings are in accordance with the study by Jelínek et al. [41]. They found that the NDVI values of wheat cultivars were higher in places with better water availability and nutrients, regardless of wheat variety.

The development of the NDVI values from the GreenSeeker was consistent with the results from the MicaSense camera. A different measurement method and a different wavelength range, as was the case in the study of Kumhálová & Matějková [23], probably caused variations in the results. They concluded that another reason of variation could be early crop scanning with different stand density. While all pixels on the parcels were taken into account from the UAV, the GreenSeeker was used only on sampling points (details in Figure 1).

The GNDVI spectral index is a reliable indicator of the chlorophyll content of the leaves. It usually has the same trend of development as NDVI [65], and this was confirmed in our study. As it can be seen in Figure 3, the stand was gradually maturing during the last date of scanning (14 July), and the chlorophyll content in the leaves was decreasing. The Kabot variety on the CT variant matures in delay, probably due to the large number of tillers.

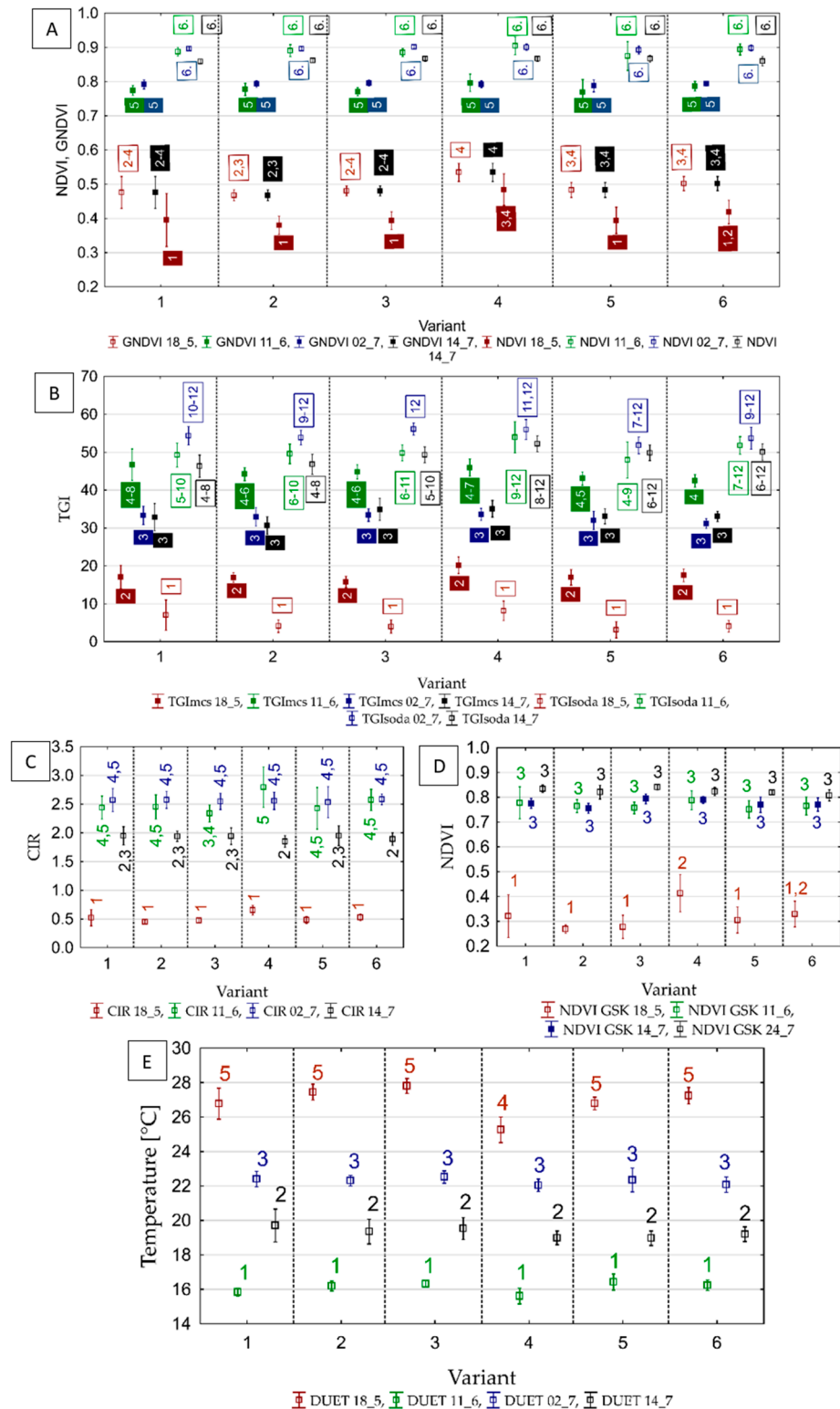


**Figure 3.** The growth parameters of selected wheat varieties under different tillage during the entire vegetation season estimated by normalized difference vegetation index (NDVI) and green NDVI (GNDVI) (A); triangular greenness index (TGI) from MicaSense (mcs) and S.O.D.A. camera (B); chlorophyll index red edge (C); NDVI from GreenSeeker (D); Thermal images from DUET camera—temperatures (°C) (E). Variants represent different types of tillage and varieties of wheat. Numbering 1,2,3... are homogenous groups according to Tukey’s HSD test,  $\alpha = 0.05$ . □, ■ Mean values for each parcel,  $I \pm 0.95$  conf. interval.

The CIR spectral index uses the red edge spectral band, which is very sensitive to the state of the cell structures of the plant tissues. The index has a very similar course to G/NDVI. However, a higher chlorophyll content on the CT plot of the Kabot variety was detected on 11 June, when the stand corresponded to the beginning of the heading growth stage. As in the case of the previously evaluated spectral indices, the reason was probably due to more beneficial soil conditions for the growth and better tillering of the Kabot variety.

The TGI index belongs to the RGB index group [66]. The TGI index was calculated from two sources—the more expensive 5 bands MicaSense RedEdge MX and the low-cost S.O.D.A. cameras. As it can be seen from Figure 3, the development of the TGI values was very similar for both data sources. The differences were probably caused due to different spectral characteristics (detail in Table 2). Both of the centers and ranges of the wavelengths of the individual bands differed. The variance of the values between the individual terms of the TGI index derived from images from the MicaSense camera was much smaller. However, as shown in Figure 3, both models of the TGI index development described the condition of the stand in the scanned terms well and are consistent with the other indices used. They are thus a very good alternative to NDVI, for example, if only an RGB camera is available. Jelínek et al. [18] solved a similar problem with spectral indices derived from two satellite images—Sentinel 2 and Landsat 8—for the evaluation of wheat varieties. Both sources were usable, but they showed slight differences.

Trends of the selected indices were in line with the content of micronutrients, especially Fe, Mn, and Zn. Although these indices are more often an indicator for the nitrogen content in the leaves or canopy structure, as described by Walsh and Shafian [67], they could be a good indicator of micronutrient content in the plant as well as in the grains. Pandey et al. [30] confirmed that the sufficient intake of micronutrients at right time and dosage can significantly increase the yield parameters of the wheat in terms of the number of spikes, height grains per spike, height of crops, among others. In the case of the selected varieties, the micronutrient content in the grains was in line with the height of both wheat varieties and affected the development of spikes in the Kabot variety. Khorasan primarily used microelements for the growth of plants and not for the development of tillers and spikes, but these micronutrients were highly concentrated in the grains themselves, which generally increased the nutritional value of the yield.

The development of canopy temperature depends on the density of the stand as well as on the other factors such as the characteristics of the thermal camera, the meteorological conditions, and the intensity of thermal radiation at the time of taking the pictures [68]. A literature review by Pandey et al. [30] that specifically focuses on the use of thermal images for the purposes of water stress detection in crops. However, the relatively high temperatures (see Figure 3) in the first campaign were affected by very sparse vegetation, such as when the bare soil was visible. The CT plot of the Kabot variety generally showed the lowest temperatures in all of the campaigns, which is in line with the results from the spectral indices. The development of temperatures has the opposite course than the used spectral indices. Thus, the results the structure of the stand.

Table 7 provides an overview of the coefficient of determination among the selected spectral indices and the measured crop and soil parameters for the Khorasan and Kabot varieties regardless of soil tillage variants. The significance of the coefficients of determination is highlighted according to Chráska [69]. It can be seen that the varieties differ in terms of their growth requirements. A significant difference between the varieties is mainly recorded in the area of spike development and grain weight and the ability of the selected spectral indices and sensors to capture details.

**Table 7.** Coefficient of determination among measured crop and soil parameters for Khorasan and Kabot varieties (level of statistical significance:  $p < 0.05$ ). Color marking: green = high dependence; red = low dependence.

	Khorasan					Kabot						
	WTS [g]	Number of Spikes [pc]	Total Weight [g]	Initial Moisture Content $\theta$ mom (Vol.%)	Bulk Density Pd ( $\text{g}\cdot\text{cm}^{-3}$ )	Total Porosity P (Vol.%)	WTS [g]	Number of Spikes [pc]	Total Weight [g]	Initial Moisture Content $\theta$ mom (Vol.%)	Bulk Density Pd ( $\text{g}\cdot\text{cm}^{-3}$ )	Total Porosity P (Vol.%)
NDVI GSK	0.82	0.22	0.41	0.01	0.07	0.54	0.39	0.81	0.82	0.10	0.19	0.37
NDVI UAV	0.63	0.41	0.57	0.13	0.26	0.24	0.44	0.81	0.73	0.35	0.35	0.18
CIR	0.45	0.49	0.63	0.27	0.26	0.31	0.34	0.73	0.65	0.34	0.48	0.12
DSM	0.61	0.55	0.79	0.30	0.31	0.38	0.44	0.86	0.77	0.27	0.24	0.28
DUET	0.66	0.50	0.66	0.21	0.25	0.37	0.60	0.77	0.75	0.25	0.20	0.36
GNDVI	0.60	0.36	0.54	0.15	0.19	0.32	0.27	0.59	0.59	0.01	0.01	0.60
Height	0.58	0.30	0.49	0.17	0.10	0.57	0.21	0.66	0.57	0.06	0.09	0.32
NDVI	0.63	0.41	0.57	0.13	0.25	0.24	0.44	0.81	0.73	0.35	0.35	0.18
TGI <sub>mcs</sub>	0.86	0.32	0.50	0.05	0.13	0.51	0.31	0.74	0.64	0.10	0.09	0.39
TGI <sub>soda</sub>	0.81	0.41	0.57	0.13	0.24	0.30	0.40	0.79	0.73	0.13	0.10	0.45

Explanation: WTS = weight of a thousand weeds; NDVI GSK = normalized different vegetation index from GreenSeeker; NDVI UAV = NDVI from unmanned aerial vehicle; CIR = chlorophyll index red edge; DSM = digital surface model; DUET = thermal image; GNDVI = green NDVI; TGI<sub>mcs</sub> = triangular greenness index from MicaSense camera; TGI<sub>soda</sub> = TGI from S.O.D.A. camera.

#### 4. Conclusions

The results showed that each tillage technology played a significant role in providing suitable conditions for the growth of Khorasan ancient wheat. Although the literature review describes that it is not a demanding crop for mountain conditions, the results of our study showed that Khorasan is better suited for the conditions of conventional tillage with moldboard plowing at 20–25 cm. A sufficient supply of both macro and micronutrients (especially Zn, Fe and Mn) can significantly positively influence the height of both wheat varieties and the development of spikes in the Kabot variety. Khorasan used micronutrients primarily for the growth of plants and not for the development of tillers and spikes. These micronutrients were then highly concentrated in the grains of the Khorasan variety in the plot with conventional tillage (with low values of bulk density and high values of total porosity), which generally increased the nutritional value of the yield in this experimental plot. An additional advantage of this variety is that it does not deplete the soil.

Our results from four types of sensors have shown the advantages of combining different data sources that can complement and emphasize details. The CIR index with the red edge spectral band highlighted the characteristics of the stand regarding the state of the canopy structure in the beginning of heading growth stage of the Kabot variety. However, the results also show that the trend of developmental growing curves derived from different sensors was very similar regardless of the measurement method (area measurement—UAV images; point measurement—GreenSeeker). Sensors used in this study can be good indicators of the micronutrient content in the plant as well as in the grains. Nevertheless, more research is needed for a more accurate confirmation of these findings. It can be concluded that a low-cost RGB camera can provide relevant results, especially in cases where equipment that is more accurate is not available.

**Author Contributions:** Conceptualization—K.B., J.M., and J.K.; methodology—K.B., J.K., and S.P.; software—J.K., J.C.; validation—J.C., J.M.; formal analysis—J.C., J.K.; investigation—K.B., J.C., and J.K.; resources—K.B., J.C., and J.K.; data curation—J.K., J.M.; writing—original draft preparation—J.K.,

K.B., and J.C.; writing—review and editing—J.K., K.B., and J.C.; visualization—J.K., J.C.; supervision—J.K., J.M. All authors have read and agreed to the published version of the manuscript.

**Funding:** This research was funded by internal project of the Faculty of Engineering at the Czech University of Life Sciences Prague, grant number 2021: 31160/1312/3111.

**Conflicts of Interest:** The authors declare no conflict of interest.

## References

- Alvarez, R.; Steinbach, H.S. A review of the effects of tillage systems on some soil physical properties, water content, nitrate availability and crops yield in the Argentine Pampas. *Soil Tillage Res.* **2019**, *104*, 1–15. [CrossRef]
- Busari, M.A.; Kukal, S.S.; Kaur, A.; Bhatt, R.; Dulazi, A.A. Conservation tillage impacts on soil, crop and environment. *Int. Soil Water Conserv. Res.* **2015**, *3*, 119–129. [CrossRef]
- Pittelkow, C.M.; Liang, X.; Linnquist, B.A.; Van Groenigen, K.J.; Lee, J.; Lundy, M.E.; Van Gestel, N.; Six, J.; Vanterea, R.T.; Van Kessel, C. Productivity limits and potentials of the principles of conservation agriculture. *Nature* **2015**, *517*, 365–368. [CrossRef] [PubMed]
- Six, J.; Feller, C.; Denef, K.; Ogle, S.; de Moraes Sa, J.C.; Albrecht, A. Soil organic matter, biota and aggregation in temperate and tropical soils—Effects of no-tillage. *Agronomie* **2002**, *22*, 755–775. [CrossRef]
- Daraghmeh, O.A.; Petersen, C.T.; Munkholm, L.J.; Znova, L.; Obour, P.B.; Nielsen, S.K.; Green, O. Impact of tillage intensity on clay loam soil structure. *Soil Use Manag.* **2019**, *35*, 388–399. [CrossRef]
- Bilalis, D.; Karkanis, A.; Patsiali, S.; Agriogianni, M.; Konstantas, A.; Triantafyllidis, V. Performance of wheat varieties (*Triticum aestivum* L.) under conservation tillage practices in organic agriculture. *Not. Bot. Horti Agrobot.* **2011**, *39*, 28–33. [CrossRef]
- Grandy, A.S.; Robertson, G.P.; Thelen, K.D. Do productivity and environmental trade-offs justify periodically cultivating no-till cropping systems? *Agron. J.* **2006**, *98*, 1377–1383. [CrossRef]
- Annicchiarico, P.; Chiapparino, E.; Perenzin, M. Response of common wheat varieties to organic and conventional production systems across Italian locations, and implications for selection. *Field Crops Res.* **2010**, *116*, 230–238. [CrossRef]
- Czech Statistical Office. Available online: <https://www.czso.cz/csu/czso/agriculture-total-a48umrqt9> (accessed on 17 June 2021).
- Šíp, V.; Růžek, P.; Chrpová, J.; Vavera, R.; Kusá, H. The effect of tillage practice, input level and environment on the grain yield of winter wheat in the Czech Republic. *Field Crops Res.* **2009**, *113*, 131–137. [CrossRef]
- Curtis, B.C. Wheat in the World 2002. Available online: <http://www.fao.org/3/y4011e/y4011e04.htm> (accessed on 18 February 2021).
- National Association of Wheat Growers 2021. Available online: <https://www.wheatworld.org/wheat-101/research/wheat-research-projects/> (accessed on 18 February 2021).
- Bordoni, A.; Danesi, F.; Di Nunzio, M.; Taccari, A.; Valli, V. Ancient wheat and health: A legend or reality? A review on KAMUT khorasan wheat. *Int. J. Food Sci. Nutr.* **2017**, *68*, 278–286. [CrossRef]
- Molberg, O.; Uhlen, A.K.; Jensen, T.; Flaete, N.S.; Fleckenstein, B.; Arentz-Hansen, H.; Raki, M.; Lundin, K.E.; Sollid, L.M. Mapping of gluten T-cell epitopes in the bread wheat ancestors: Implications for celiac disease. *Gastroenterology* **2005**, *128*, 393–401. [CrossRef]
- Trozzi, C.; Raffaelli, F.; Vignini, A.; Nanetti, L.; Gesuita, R.; Mazzanti, L. Evaluation of antioxidative and diabetes-preventive properties of an ancient grain, KAMUT® khorasan wheat in healthy volunteers. *Eur. J. Nutr.* **2019**, *58*, 151–161. [CrossRef]
- Quinn, R.M. Kamut®: Ancient grain, new cereal. In *Perspectives on New Crops and New Uses*; Janick, J., Ed.; ASHS Press: Alexandria, VA, USA, 1999; pp. 182–183.
- Kumhálová, J.; Zemek, F.; Novák, P.; Brovkina, O.; Mayerová, M. Use of Landsat images for yield evaluation within a small plot. *Plant Soil Environ.* **2014**, *60*, 501–506. [CrossRef]
- Jelínek, Z.; Kumhálová, J.; Chyba, J.; Wohlmuthová, M.; Madaras, M.; Kumhála, F. Landsat and Sentinel-2 images as a tool for the effective estimation of winter and spring cultivar growth and yield prediction in the Czech Republic. *Int. Agrophys.* **2020**, *34*, 391–406. [CrossRef]
- Chemura, A.; Mutanga, O.; Dube, T. Separability of coffee leaf rust infection levels with machine learning methods at Sentinel-2 MSI spectral resolutions. *Precis. Agric.* **2017**, *18*, 859–881. [CrossRef]
- Comba, L.; Gay, P.; Primicerio, J.; Aimonino, D.R. Vineyard detection from unmanned aerial systems images. *Comput. Electron. Agric.* **2015**, *114*, 78–87. [CrossRef]
- Maes, W.H.; Steppe, K. Perspectives for Remote Sensing with Unmanned Aerial Vehicles in Precision Agriculture. *Trends Plant Sci.* **2019**, *24*, 152–164. [CrossRef]
- Ali, A.M.; Ibrahim, S.M. Wheat grain yield and nitrogen uptake prediction using Leaf and GreenSeeker portable optical sensors at jointing growth stage. *Inf. Proc. Agric.* **2020**, *7*, 375–383.
- Kumhálová, J.; Matějková, Š. Yield variability prediction by remote sensing sensors with different spatial resolution. *Int. Agrophys.* **2017**, *31*, 195–2020. [CrossRef]
- Naser, M.A.; Khosla, R.; Longchamps, L.; Dahal, S. Using NDVI to Differentiate Wheat Genotypes Productivity under Dryland and Irrigated Conditions. *Remote Sens.* **2020**, *12*, 824. [CrossRef]

25. Viña, A.; Gitelson, A.A.; Nguy-Robertson, A.L.; Peng, Y. Comparison of different vegetation indices for the remote assessment of green leaf area index of crops. *Remote Sens. Environ.* **2011**, *115*, 3468–3478. [CrossRef]
26. Stroppiana, D.; Bordogna, G.; Carrara, P.; Boschetti, M.; Boschetti, L.; Brivio, P.A. A method for extracting burned areas from Landsat TM/ETM+ images by soft aggregation of multiple Spectral Indices and a region growing algorithm. *ISPRS J. Photogramm. Remote Sens.* **2012**, *69*, 88–102. [CrossRef]
27. Chlingaryan, A.; Sukkariéh, S.; Whelan, B. Machine learning approaches for crop yield prediction and nitrogen status estimation in precision agriculture: A review. *Comput. Electron. Agric.* **2018**, *151*, 61–69. [CrossRef]
28. Su, J.; Liu, C.; Coombes, M.; Hu, X.; Wang, C.; Xu, X.; Li, Q.; Guo, L.; Chen, W.H. Wheat yellow rust monitoring by learning from multispectral UAV aerial imagery. *Comput. Electron. Agric.* **2018**, *155*, 157–166. [CrossRef]
29. Pádua, L.; Marques, P.; Adão, T.; Guimarães, N.; Sousa, A.; Peres, E.; Sousa, J.J. Vineyard Variability Analysis through UAV-Based Vigour Maps to Assess Climate Change Impacts. *Agronomy* **2019**, *9*, 581. [CrossRef]
30. Pandey, M.; Shresthab, J.; Subedic, S.; Shahd, K.K. Role of nutrients in wheat: A review. *Trop. Agrobiodivers.* **2020**, *1*, 18–23. [CrossRef]
31. Gago, J.; Douthe, C.; Coopman, R.E.; Gallego, P.P.; Ribas-Carbo, M.; Flexas, J.; Escalona, J.; Medrano, H. UAVs challenge to assess water stress for sustainable agriculture. *Agric. Water Manag.* **2015**, *153*, 9–19. [CrossRef]
32. Khan, A.; Upadhyay, C.S.; Gerritsma, M. Spectral element method for parabolic interface problems. *Comput. Methods Appl. Mech. Eng.* **2018**, *337*, 66–94. [CrossRef]
33. Rouse, J.; Haas, R.; Schell, J.A.; Deering, D. Monitoring vegetation systems in the Great Plains with ERTS. In Proceedings of the Third ERTS-1 Symposium, NASA SP-351, Washington, DC, USA, 10–14 December 1973; pp. 309–317.
34. Heumann, B.W.; Seaquist, J.W.; Eklundh, L.; Jönsson, P. AVHRR derived phenological change in the Sahel and Soudan. Africa. 1982–2005. *Remote Sens. Environ.* **2007**, *108*, 385–392. [CrossRef]
35. Fu, Z.; Jiang, J.; Gao, Y.; Krienke, B.; Wang, M.; Zhong, K.; Cao, Q.; Tian, Y.; Zhu, Y.; Cao, W.; et al. Wheat Growth Monitoring and Yield Estimation based on Multi-Rotor Unmanned Aerial Vehicle. *Remote Sens.* **2020**, *12*, 508. [CrossRef]
36. Kamenova, I.; Dimitrov, P. Evaluation of Sentinel-2 vegetation indices for prediction of LAI, fAPAR and fCover of winter wheat in Bulgaria. *Eur. J. Remote Sens.* **2020**, *54*, 89–108. [CrossRef]
37. Domínguez, J.A.; Kumhálová, J.; Novák, P. Winter oilseed rape and winter wheat growth prediction using remote sensing methods. *Plant Soil Environ.* **2015**, *61*, 410–416.
38. Gitelson, A.A.; Kaufman, Y.; Merzlyak, M.N. Use of green channel in remote sensing of global vegetation from EOS-MODIS. *Remote Sens. Environ.* **1996**, *58*, 289–298. [CrossRef]
39. Frampton, W.J.; Dash, J.; Watmough, G.; Milton, E.J. Evaluating the capabilities of Sentinel-2 for quantitative estimation of biophysical variables in vegetation. *ISPRS J. Photogramm. Remote Sens.* **2013**, *82*, 83–92. [CrossRef]
40. Hunt, E.R.; Doraiswamy, P.C.; McMurtrey, J.E.; Daughtry, C.S.T.; Perry, E.M.; Akhmedov, B. A Visible Band Index for Remote Sensing Leaf Chlorophyll Content at the Canopy Scale. *Int. J. Appl. Earth Observ. Geoinf.* **2013**, *21*, 103–112. [CrossRef]
41. Jelínek, Z.; Starý, K.; Kumhálová, J.; Lukáš, J.; Mašek, J. Winter wheat, winter rape and poppy crop growth evaluation with the help of remote and proximal sensing measurements. *Agron. Res.* **2020**, *18*, 2049–2059.
42. Gitelson, A.; Merzlyak, M.N. Spectral reflectance changes associated with autumn senescence of *Aesculus hippocastanum* L. and *Acer platanoides* L. leaves. Spectral features and relation to chlorophyll estimation. *J. Plant Physiol.* **1994**, *143*, 286–292. [CrossRef]
43. Xie, Q.; Dash, J.; Huang, W.; Peng, D.; Qin, Q.; Mortimer, H.; Casa, R.; Pignatti, S.; Laneve, G.; Pascucci, S.; et al. Vegetation Indices Combining the Red and Red-Edge Spectral Information for Leaf Area Index Retrieval. *IEEE J. Sel. Top. Appl. Earth Observ. Remote Sens.* **2018**, *11*, 1482–1493. [CrossRef]
44. Gitelson, A.A.; Gritz, Y.; Merzlyak, M.N. Relationships between leaf chlorophyll content and spectral reflectance and algorithms for nondestructive chlorophyll assessment in higher plant leaves. *J. Plant Physiol.* **2003**, *160*, 271–282. [CrossRef] [PubMed]
45. Boegh, E.; Soegaard, H.; Broge, N.; Hasager, C.; Jensen, N.; Schelde, K.; Thomsen, A. Airborne Multi-spectral Data for Quantifying Leaf Area Index, Nitrogen Concentration and Photosynthetic Efficiency in Agriculture. *Remote Sens. Environ.* **2002**, *81*, 179–193. [CrossRef]
46. Gitelson, A.A.; Vina, A.; Ciganda, V.; Rundquist, D.C.; Arkebauer, T.J. Remote estimation of canopy chlorophyll content in crops. *Geophys. Res. Lett.* **2005**, *32*, L08403. [CrossRef]
47. Potter, C.; Li, S.; Huang, S.; Crabtree, R.L. Analysis of sapling density regeneration in Yellowstone National Park with hyperspectral remote sensing data. *Remote Sens. Environ.* **2012**, *121*, 61–68. [CrossRef]
48. Dash, J.; Curran, P.J. The MERIS terrestrial chlorophyll index. *Int. J. Remote Sens.* **2004**, *25*, 5403–5413. [CrossRef]
49. Bleiholder, H.T.; Boom, V.D.; Langelüdecke, P.; Stauss, R. Einheitliche Codierung der phänologischen Stadien bei Kultur und Schädelpflanzen. *Gesunde Pflanz.* **1989**, *41*, 381–384.
50. GreenSeeker Handheld Crop Sensor. Trimble Inc. 2021. Available online: <https://agriculture.trimble.com/product/greenseeker-handheld-crop-sensor/> (accessed on 11 March 2021).
51. Valla, M.; Kozák, J.; Němeček, J.; Matula, S.; Borůvka, L.; Drábek, O. *Pedological Practicum (Pedologické Praktikum)*, 2nd ed.; Czech University of Life Sciences Prague: Prague, Czech Republic, 2011; p. 155. (In Czech)
52. Mehlich, A. Mehlich 3 soil test extractant: A modification of Mehlich 2 extractant. *Commun. Soil Sci. Plant Anal.* **1984**, *15*, 1409–1416. [CrossRef]

53. Trávník, K.; Zbiral, J.; Němec, P. *Agrochemical Testing of Agricultural Soils—Mehlich III (Agrochemické Zkoušení Zemědělských Půd—Metoda Mehlich III)*, 1st ed.; Central Institute for Supervision and Testing in Agriculture: Brno, Czech Republic, 1999; p. 100. (In Czech)
54. Mühlbachová, G.; Čermák, P.; Káš, M.; Vavera, R.; Pechova, M.; Marková, K. Boron content in soils under increasing magnesium and sulphur doses in a field experiment. *Plant Soil Environ.* **2020**, *66*, 366–373. [[CrossRef](#)]
55. Ikanović, J.; Popović, V.; Janković, S.; Živanović, L.; Rakić, S.; Dončić, D. Khorasan wheat population researching (*Triticum turgidum*, ssp. *Turanicum* (McKey) in the minimum tillage conditions. *Genetika* **2014**, *46*, 105–115. [[CrossRef](#)]
56. Wijngaard, H.; Arendt, E.K. Buckwheat. *Cereal Chem.* **2006**, *83*, 391–401. [[CrossRef](#)]
57. Slavin, J.L.; Jacobs, D.; Marquart, L. Grain processing and nutrition. *Crit. Rev. Food Sci. Nutr.* **2000**, *40*, 309–326. [[CrossRef](#)] [[PubMed](#)]
58. Maki, K.C.; Phillips, A.K. Dietary substitutions for refined carbohydrate that show promise for reducing risk of type 2 diabetes in men and women. *J. Nutr.* **2015**, *145*, 159S–163S. [[CrossRef](#)]
59. Grausgruber, H.; Oberforster, M.; Ghambashidze, G.; Ruckenbauer, P. Yield and agronomic traits of Khorasan wheat (*Triticum turanicum* Jakubz.). *Field Crops Res.* **2005**, *91*, 319–327. [[CrossRef](#)]
60. Tari, A.F. The effects of different deficit irrigation strategies on yield, quality, and water-use efficiencies of wheat under semi-arid conditions. *Agric. Water Manag.* **2016**, *167*, 1–10. [[CrossRef](#)]
61. Michalcová, V.; Dušínský, R.; Sabo, M.; Al Beyroutiová, M.; Hauptvogel, P.; Ivaničová, Z.; Švec, M. Taxonomical classification and origin of Kamut® wheat. *Plant Syst. Evol.* **2014**, *300*, 1749–1757. [[CrossRef](#)]
62. Bendig, J.; Yu, K.; Aasen, H.; Bolten, A.; Bennertz, S.; Broscheit, J.; Gnyp, M.L.; Bareth, G. Combining UAV-based plant height from crop surface models, visible, and near infrared vegetation indices for biomass monitoring in barley. *Int. J. Appl. Earth Observ. Geoinf.* **2015**, *39*, 79–87. [[CrossRef](#)]
63. Glamoclija, D.; Jankovic, S.; Pivic, R. *Alternative of Rye (Alternativna Žita)*; Institute of Soil Science: Belgrade, Serbia, 2012; pp. 1–30. (In Polish)
64. Rajičić, V.; Popović, V.; Perišić, V.; Biberdžić, M.; Jovović, Z.; Gudžić, N.; Mihailović, V.; Čolić, V.; Đurić, N.; Terzić, D. Impact of nitrogen and phosphorus on grain yield in winter triticale grown on degraded Vertisol. *Agronomy* **2020**, *10*, 757. [[CrossRef](#)]
65. Gitelson, A.A.; Kaufman, Y.J.; Stark, R.; Rundquist, D. Novel Algorithms for Remote Estimation of Vegetation Fraction. *Remote Sens. Environ.* **2002**, *80*, 76–87. [[CrossRef](#)]
66. Mckinnon, T.; Hoff, P. Comparing RGB-based vegetation indices with NDVI for drone based agricultural sensing. *Agribotix* **2017**, *21*, 1–8.
67. Walsh, S.O.; Shafian, S. Assessment of Red-Edge based vegetation indices derived from unmanned aerial vehicle for plant nitrogen content estimation. In Proceedings of the 14th International Conference on Precision Agriculture, Montreal, QC, Canada, 24–27 June 2018.
68. Khanal, S.; Fulton, J.; Shearer, S. An overview of current and potential applications of thermal remote sensing in precision agriculture. *Comput. Electron. Agric.* **2017**, *139*, 22–32. [[CrossRef](#)]
69. Chráska, M. *Basics of Research in Pedagogy (Základy Výzkumu v Pedagogice)*, 2nd ed.; Palacký University: Olomouc, Czech Republic, 1998; p. 257. (In Czech)